

Research Paper

Prediction of Human Drug Clearance from *in Vitro* and Preclinical Data Using Physiologically Based and Empirical Approaches

Kiyomi Ito¹ and J. Brian Houston^{1,2}

Received April 12, 2004; accepted September 13, 2004

Purpose. The aim of this study is to compare the accuracy of five methods for predicting *in vivo* intrinsic clearance (CL_{int}) and seven for predicting hepatic clearance (CL_h) in humans using *in vitro* microsomal data and/or preclinical animal data.

Methods. The human CL_{int} was predicted for 33 drugs by five methods that used either *in vitro* data with a physiologic scaling factor (SF), with an empirical SF, with the physiologic and drug-specific (the ratio of *in vivo* and *in vitro* CL_{int} in rats) SFs, or rat CL_{int} directly and with allometric scaling. Using the estimated CL_{int} , the CL_h in humans was calculated according to the well-stirred liver model. The CL_h was also predicted using additional two methods: using direct allometric scaling or drug-specific SF and allometry.

Results. Using *in vitro* human microsomal data with a physiologic SF resulted in consistent underestimation of both CL_{int} and CL_h . This bias was reduced by using either an empirical SF, a drug-specific SF, or allometry. However, for allometry, there was a substantial decrease in precision. For drug-specific SF, bias was less reduced, precision was similar to an empirical SF. Both CL_{int} and CL_h were best predicted using *in vitro* human microsomal data with empirical SF. Use of larger data set of 52 drugs with the well-stirred liver model resulted in a best-fit empirical SF that is 9-fold increase on the physiologic SF.

Conclusions. Overall, the empirical SF method and the drug-specific SF method appear to be the best methods; they show lower bias than the physiologic SF and better precision than allometric approaches. The use of *in vitro* human microsomal data with an empirical SF may be preferable, as it does not require extra information from a preclinical study.

KEY WORDS: allometry; clearance prediction; hepatic clearance; intrinsic clearance, *in vitro* scaling.

INTRODUCTION

Several approaches have been advocated to predict drug clearance in humans that involve the use of *in vitro* human microsomal data and/or preclinical animal data. *In vitro* drug metabolism kinetic parameters can provide an estimate of *in vivo* intrinsic clearance (CL_{int}) for the whole liver by the use of a scaling factor (SF) and subsequently hepatic clearance (CL_h) with the use of a liver model (1). Physiologically based

scaling factors (PB-SF) are preferred, for example, hepatocellularity for isolated hepatocytes, and for microsomes a SF accounting for incomplete microsomal recovery from human liver tissue based on CYP content in homogenate and microsomes (1–3). Alternative approaches to the use of *in vitro* data have also been suggested for the prediction of human drug clearances that use preclinical animal data; these include the use of allometry (4–8), drug-specific factors based on rat *in vitro* and *in vivo* parameters (9), as well as considering a combination of both of the above (10,11). In addition, some of the investigators have suggested the possibility of ignoring drug binding within the plasma and microsomal matrices on the grounds that, if identical, these parameters will cancelled out when liver models are applied (7).

The aim of this study was to investigate the full spectrum of these different approaches and make direct comparisons of their accuracy and precision for predicting human *in vivo* clearances with a much larger data set ($n = 52$) than that used in previous studies (3,7,11). *In vitro* CL_{int} data were taken from published human and rat microsomal studies while comparable *in vivo* CL_{int} were calculated via the well-stirred liver model from published CL_h data. Data for 33 drugs were used to compare five different approaches for predicting CL_{int} and seven approaches for predicting CL_h . PB approaches are compared to several empirical approaches using regression analysis, allometry, or preclinical *in vivo* data either alone or

¹ School of Pharmacy and Pharmaceutical Sciences, University of Manchester, Manchester M13 9PL, UK.

² To whom correspondence should be addressed. (e-mail: Brian.Houston@man.ac.uk)

ABBREVIATIONS: *afe*, average fold-error; B_h , mean body weights of humans; B_r , mean body weights of rats; $CL_{h,h}$, hepatic clearance in humans; $CL_{h,r}$, hepatic clearance in rats; CL_{int} , intrinsic clearance; CL_h , hepatic clearance; $CL_{int,h,in vitro}$, *in vitro* intrinsic clearance in humans; $CL_{int,h,in vivo}$, *in vivo* intrinsic clearance in humans; $CL_{int,r,in vitro}$, *in vitro* intrinsic clearance in rats; $CL_{int,r,in vivo}$, *in vivo* intrinsic clearance in rats; f_u,p , plasma unbound fraction; f_u,m , unbound fraction in microsomes; K_a , affinity constant for the protein; K_a,m , affinity constant for drug binding in microsomes; K_a,p , affinity constant for drug binding in plasma; *mse*, mean squared prediction error; P , protein concentration; PB-SF, physiologically based SF; Q_h , hepatic blood flow; R_B , blood-to-plasma concentration ratio; *rmse*, root mean squared prediction error; SF, scaling factor.

in combination with *in vitro* data for specific drugs. For CL_h estimation, direct prediction and prediction via the use of CL_{int} and a liver model is compared. In addition, the consequences of nonspecific drug binding is investigated, both in the incorporation of plasma binding in liver models and the impact of relative drug binding within plasma and microsomal matrices using data for 46 drugs.

MATERIALS AND METHODS

Data Collection

In vitro intrinsic clearance in humans ($CL_{int,h,in vitro}$) was obtained from published metabolic studies using human liver microsomes. *In vivo* intrinsic clearance in humans ($CL_{int,h,in vivo}$) was calculated from the published values of CL_h , plasma unbound fraction (f_u,p), and blood-to-plasma concentration ratio (R_B) for each drug according to the well-stirred liver model as follows:

$$CL_{int,h,in vivo} = Q_h \times CL_h / (Q_h - CL_h) / (f_u,p / R_B) \quad (1)$$

where Q_h represents the hepatic blood flow (20.7 ml min⁻¹ kg⁻¹). These values for humans were available for 52 drugs (see Table I).

The *in vitro* and *in vivo* intrinsic clearances in rats ($CL_{int,r,in vitro}$ and $CL_{int,r,in vivo}$, respectively) were also obtained for 33 drugs (no. 1-33 in Table I) in a similar manner as those for humans except that Q_h of 100 (ml min⁻¹ kg⁻¹) was used.

For the human data, *in vivo* intrinsic clearances were also calculated using the assumptions of the parallel-tube liver model as follows:

$$CL_{int,h,in vivo} = -Q_h / (f_u,p / R_B) \times \ln(1 - CL_h / Q_h) \quad (2)$$

The assumptions of both the well-stirred and parallel-tube liver models have been previously discussed (27). Blood flow estimates were based on published values for human (28,29) and rat (30,31). It should be noted that the higher the clearance value, the more sensitive the CL_{int} calculation is to the blood flow value used.

Prediction of the *in Vivo* Intrinsic Clearance

$CL_{int,h,in vivo}$ (ml min⁻¹ kg⁻¹) for the 33 drugs for which rat data were available was predicted using the following five methods (A–E) and compared with the observed CL_{int} values calculated from CL_h as described above.

A. Using a Physiologically Based Scaling Factor

This method uses human microsomal data and a physiologically based scaling factor (PB-SF) based on hepatic microsomal recovery from the whole liver for conversion of the unit of the CL_{int} from ml min⁻¹ mg⁻¹ protein to ml min⁻¹ kg⁻¹ (1).

$$CL_{int,h,in vivo} = CL_{int,h,in vitro} \text{ (ml/min/mg protein)} \times \text{PB-SF} \quad (3)$$

where the PB-SF (856 ± 270 mg protein/kg) is the average recovery ± SD of microsomal protein per gram of liver (40 mg protein/g liver) determined using 38 human livers (Hakooz *et al.*, unpublished observation) multiplied by the average liver weight in humans (21.4 g liver/kg).

B. Using an Empirical Scaling Factor

This method uses human microsomal data and an empirical SF of 6.2 (SD 0.2)g protein/kg body weight as a substitute for PB-SF and takes into account the extent of under-prediction associated with using method A. The empirical SF was determined by the regression analysis to obtain the best fit of $CL_{int,h,in vivo}$ and $CL_{int,h,in vitro}$ values using an equation analogous to Eq. 3. The leave-one-out approach was used and the average coefficient taken as the empirical SF.

C. Physiologically Based and Drug-Specific Scaling Factors

Like method A, this approach uses human microsomal data and PB-SF plus a drug specific factor based on *in vivo* and *in vitro* CL_{int} in rats (both in the unit of ml min⁻¹ kg⁻¹) (9).

$$CL_{int,h,in vivo} = CL_{int,h,in vitro} \times \text{PB-SF} \times (CL_{int,r,in vivo} / CL_{int,r,in vitro}) \quad (4)$$

where $CL_{int,r,in vitro}$ (ml min⁻¹ kg⁻¹) was calculated using the scaling factor of 500 (mg protein/250 g) (2).

D. Rat Intrinsic Clearance

No scaling factors are used in this approach, only *in vivo* rat data (ml min⁻¹ kg⁻¹).

$$CL_{int,h,in vivo} = CL_{int,r,in vivo} \quad (5)$$

E. Using Allometric Scaling

As in D, this method uses rat *in vivo* data but also involves an allometric factor (4,5).

$$CL_{int,h,in vivo} = CL_{int,r,in vivo} \times (B_h / B_r)^x \quad (6)$$

where B_h and B_r are the mean body weights of humans (70 kg) and rats (250 g), respectively. The exponent (x) for each individual drug was determined by Eq. 7, which is re-arranged from Eq. 6 using the observed values of $CL_{int,h,in vivo}$.

$$x = \log(CL_{int,h,in vivo} / CL_{int,r,in vivo}) / \log(B_h / B_r) \quad (7)$$

The average exponent (x) for all drugs excluding the drug under study is then used for the allometric scaling of individual drugs ($x = 0.538 \pm 0.293$).

Prediction of the Hepatic Clearance

Using the *in vivo* intrinsic clearance calculated above, the hepatic clearance in humans ($CL_{h,h}$) was calculated (methods A–E) according to the “well-stirred” liver model as follows:

$$CL_{h,h} = Q_h \times f_u,p / R_B \times CL_{int,h,in vivo} / (Q_h + f_u,p / R_B \times CL_{int,h,in vivo}) \quad (8)$$

where Q_h of 20.7 (ml min⁻¹ kg⁻¹) was used as above.

The $CL_{h,h}$ was also directly calculated using the following two methods.

F. Direct Allometric Scaling

For this approach, rat hepatic clearance ($CL_{h,r}$) data are used directly with an allometric factor (8).

$$CL_{h,h} = CL_{h,r} \times (B_h / B_r)^y \quad (9)$$

Table I. Values of Intrinsic Clearance in Humans and Rats

No.	Drugs ^a	Human CL _{int} (ml min ⁻¹ kg ⁻¹)		Rat CL _{int} (ml min ⁻¹ kg ⁻¹)	
		<i>in vitro</i>	<i>in vivo</i>	<i>in vitro</i>	<i>in vivo</i>
1	FK1052 ⁹	40	1600	1100	28,000
2	FK480 ⁹	51	340	250	5700
3	Zolpidem ⁹	20	160	170	730
4	Omeprazole ⁹	67	520	650	5700
5	Nicardipine ⁹	1200	1900	13,000	14,000
6	Nilvadipine ⁹	1200	8400	72,000	240,000
7	Diazepam ⁹	10	21	500	760
8	Diltiazem ⁹	81	300	730	1600
9	Diazepam ²	4.1	13	220	1300
10	Midazolam	44	270	220	1000
11	Triazolam	13	38	340	1600
12	Flunitrazepam	5.0	11	240	380
13	Alprazolam	2.0	3.1	470	1300
14	Phenytoin ^{2,12}	0.16	4.0	92	220
15	Tolbutamide ^{2,12}	1.2	2.0	16	6.0
16	Ibuprofen ^{1,12}	8.2	83	77	240
17	Diclofenac ^{12,13}	35	630	280	670
18	Imipramine ^{1,14}	18	310	9000	7500
19	Warfarin ^{2,14}	0.49	4.5	9.1	20
20	Hexobarbital ^{1,14}	2.2	8.2	870	320
21	Dofetilide ^{2,3}	0.40	4.5	36	96
22	Metoprolol ^{1,3}	18	26	88	680
23	Phenacetin ^{1,3}	19	46	66	520
24	s-Warfarin ^{2,3}	1.0	5.7	4.2	16
25	r-Warfarin ^{2,3}	0.15	5.4	14	24
26	YW796 ¹⁵	15	14	1700	4800
27	Indinavir ¹⁶⁻¹⁸	16	130	140	570
28	Lidocaine ^{1,8,19}	3.1	55	400	2500
29	Ondansetron ^{2,8,20}	1.7	33	850	630
30	Antipyrine ^{1,11,21}	0.14	0.51	7.2	6.0
31	Caffeine ^{2,11,22}	0.43	3.5	11	14
32	Felodipine ^{1,11,23}	98	4300	1000	440
33	Propranolol ^{11,24-26}	90	340	8600	41000
34	Chlorpromazine ¹⁴	24	370		
35	Propafenone ¹⁴	160	4000		
36	Verapamil ¹⁴	120	1800		
37	Diphenhydramine ¹⁴	2.0	52		
38	Lorcanide ¹⁴	48	710		
39	Amitriptyline ¹⁴	13	490		
40	Desipramine ¹⁴	16	150		
41	Ketamine ¹⁴	26	550		
42	Quinidine ¹⁴	3.2	22		
43	Clozapine ¹⁴	4.4	59		
44	Dexamethasone ¹⁴	2.9	14		
45	Prednisone ¹⁴	2.6	21		
46	Methoxsalen ¹⁴	38	1000		
47	Tenidap ¹⁴	7.9	80		
48	Tenoxicam ¹⁴	1.6	2.2		
49	Amobarbital ¹⁴	0.89	1.4		
50	Methohexital ¹⁴	47	180		
51	Mexiletine ³	0.77	26		
52	Theophylline ³	0.033	3.5		

^a Reference source given after drug name.

The exponent (y) for each individual drug was determined by Eq. 10, which is re-arranged from Eq. 9 using the observed values of CL_{h,h}.

$$y = \log (CL_{h,h}/CL_{h,r})/\log (B_h/B_r) \quad (10)$$

The average exponent (y) for all drugs excluding the drug

under study is then used for the allometric scaling of individual drugs ($y = 0.616 \pm 0.190$).

G. A Drug-Specific Scaling Factor and Allometry

This method uses rat hepatic clearance data directly with both an allometric factor and the drug specific factor outlined in method C (10,11).

$$CL_{h,h} = CL_{h,r} \times (CL_{int,h,in\ vitro}/CL_{int,r,in\ vitro}) \times (B_h/B_r)^z \quad (11)$$

The exponent (z) for each individual drug was determined by Eq. 12, which is re-arranged from Eq. 11 using the observed values of $CL_{h,h}$.

$$z = \log (CL_{h,h}/CL_{h,r} \times CL_{int,r,in\ vitro}/CL_{int,h,in\ vitro}) / \log (B_h/B_r) \quad (12)$$

The average exponent (z) for all drugs excluding the drug under study is then used for the allometric scaling of individual drugs ($z = 1.23 \pm 0.23$). The predicted $CL_{h,h}$ values were replaced by the value of Q_h (20.7 ml/min/kg) when they were above Q_h (5 out of 33 cases).

Accuracy of Predictions

The accuracy of the predictions was assessed from the prediction error (difference between predicted and observed *in vivo* values) for each drug in a particular *in vitro* system. For visual inspection this was plotted as the log of the ratio of predicted/observed clearance against the predicted clearance (2) and the limits of ± 0.3 represented a 2-fold error. For the $CL_{int,h,in\ vitro}$, the predicted/observed clearance ratio was calculated directly and for CL_h predictions, the error in CL_{int} was propagated through the liver model calculation. Both 2- and 3-fold error limits were propagated.

Also the accuracy of each prediction method was compared from the root mean squared prediction error (*rmse*) and the average fold-error (*afe*) as measures of precision and bias, respectively, estimated as follows (7,32):

$$afe = 10^{\frac{1}{N} \sum \log \frac{\text{Predicted}}{\text{Observed}}} \quad (13)$$

$$mse = \frac{1}{N} \sum (\text{Predicted} - \text{Observed})^2, \quad rmse = \sqrt{mse} \quad (14)$$

The variance of the prediction is calculated from the sum of the squares of the prediction errors and this provides the *rmse*. The geometric mean of the prediction error provides a measure of bias with equal value to under- and over-predictions in the form of *afe*.

The correlation analyses were also performed between the predicted and observed values for each parameter to obtain the squared correlation coefficient (r^2).

Impact of Ignoring Protein Binding

In *in vitro* liver microsomal studies, some drugs bind non-specifically within the matrix, hence the kinetic parameters estimated need to be corrected to reflect the unbound drug. On the other hand, in the equations for liver models, drug binding in blood and microsomes would theoretically cancel out if the unbound fraction (fu) is the same for blood and microsomes (7):

$$CL_h = Q_h \times fu,p/R_B \times (CL_{int}/fu,m)/(Q_h + fu,p/R_B \times (CL_{int}/fu,m)) \quad (15)$$

where fu,m is the unbound fraction in microsomes.

The validity of this assumption was investigated by the following two approaches. Firstly, the human $CL_{int,h,in\ vitro}$ values for the above-mentioned 52 drugs were calculated according to the Eq. 16, modified from Eq. 1, ignoring the plasma protein binding:

$$CL_{int,h,in\ vitro} = Q_h \times CL_h / (Q_h - CL_h) \quad (16)$$

The calculated values of $CL_{int,h,in\ vitro}$ were then compared with the values predicted using the PB-SF (Eq. 3).

In the second approach, the fu for both human plasma and human liver microsomes were collected from literature (9,14,33) or obtained in our laboratory (unpublished observation). 46 drugs in total were classified into basic, neutral, and acidic drugs, depending on their charge at physiologic pH. The fu of a drug can be expressed by the following equation, using the affinity constant for tissue macromolecules, e.g., protein, (K_a) and tissue macromolecules (binding site) concentration (P):

$$fu = 1/(1 + K_a P) \quad (17)$$

In plasma the average albumin concentration is 40 mg/ml. The fu,m values are normally measured at the microsomal concentration used in the metabolism study, which differs with substrate used and laboratory. Therefore for each drug the fu,m at the protein concentration of 1 mg/ml was estimated using Eq. 17 and using the reported values of P . If the K_a for microsomes ($K_{a,m}$) is assumed to be proportional to that for plasma ($K_{a,p}$) ($K_{a,m}/K_{a,p} = a$), the equation for fu,p at $p = 40$ mg/ml and that for fu,m at $p = 1$ mg/ml can be combined to give the following equation:

$$fu,m = 40 fu,p / \{a + (40 - a) fu,p\} \quad (18)$$

The relationship between fu,m and fu,p was analyzed based on Eq. 18.

RESULTS

Prediction of the *in Vivo* Intrinsic Clearance

Figures 1A–1E illustrate the correlations between the observed and predicted values of $CL_{int,h,in\ vitro}$ using each of the five methods. In order to assess the accuracy and bias of the predictions, the prediction error (expressed as the log of the predicted/observed clearance ratio) were plotted as a function of predicted clearance (Fig. 2) and various statistical parameters calculated (Table II).

Human microsomal data in combination with the PB-SF (method A) resulted in a strong correlation ($r^2 = 0.82$) but a general underprediction of CL_{int} (Fig. 1A). The bias in this method was reduced by the introduction of either an empirical SF (method B) or a drug-specific factor (the ratio of *in vivo* and *in vitro* CL_{int} obtained in rats—method C), see Table II. There is no in bias when rat *in vivo* data are used with the allometric factor (method E) which is marked better than using rat *in vivo* data alone (method D). However method E, in comparison to methods B and C, is associated with the poorest precision and the lowest r^2 of these predictions (Fig. 1E, Table II) when considered relative to the PB-SF (method A).

Prediction of the Hepatic Clearance

CL_h were predicted using the well-stirred liver model and the $CL_{int,h,in\ vitro}$ values calculated from each of the five methods (A–E) described above. In addition two other methods (F and G) were also used to predict CL_h directly, either using allometry alone or in combination with a drug specific factor. Graphical comparisons of the prediction methods are

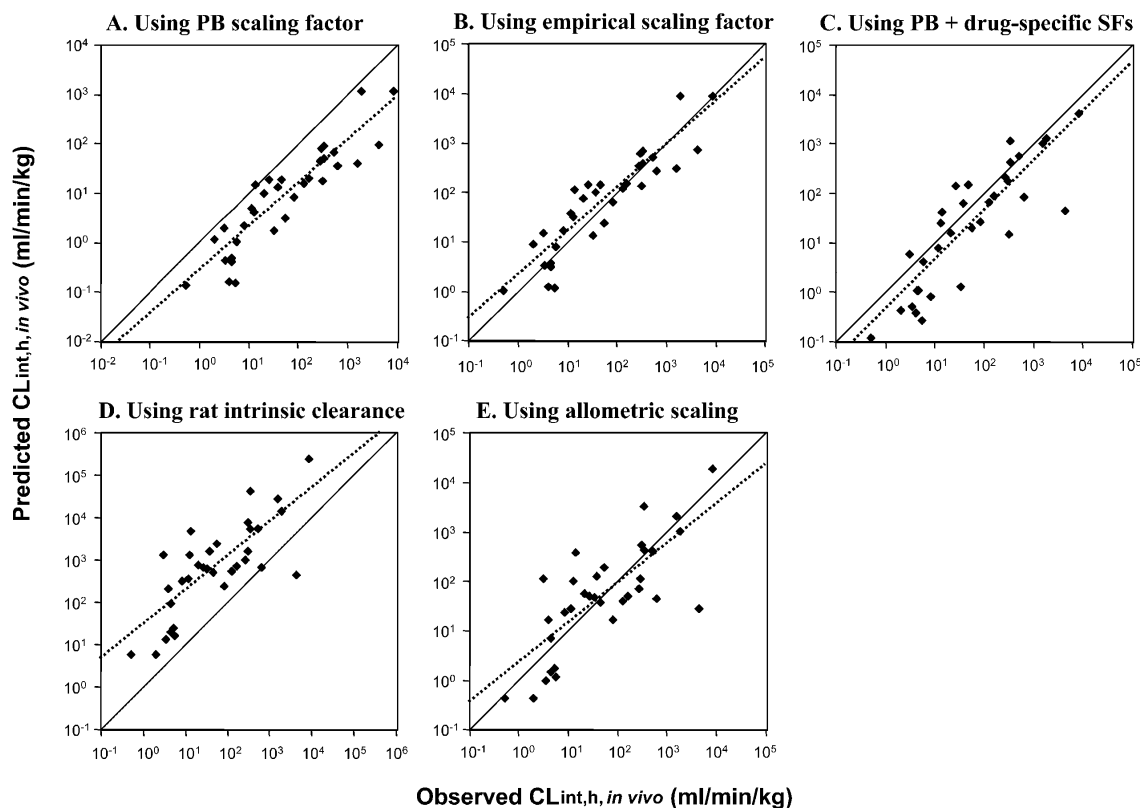


Fig. 1. Correlation between the observed and predicted human CL_{int} for 33 drugs determined using the five different approaches. (A) Using PB-SF, (B) using empirical SF, (C) using PB-SF and drug-specific SF, (D) rat intrinsic clearance, and (E) using allometric scaling. Lines represent the regression (dotted line) and unity (solid line).

shown in Fig. 3 and the parameters for the accuracy of predictions are summarized in Table II.

Similar trends for CL_h predictions for methods A–E were seen to that discussed above for CL_{int} (see Fig. 3, method D not shown). Prediction of CL_h directly by allometry (method F, Fig. 3F) showed low bias but poor precision and a particularly low r^2 . Incorporation of a drug specific factor (method G, Fig. 3G) did little to improve this approach. If Q_h did not restrict the predicted CL_h values (i.e. if the values above 20.7 ml/min/kg were allowed, 5 out of the 33 cases) in method G, the value of $rmse$ is increased to 19.2 and the r^2 is reduced to 0.154. These characteristics are clearly illustrated in the precision error for CL_h as shown in Fig. 4.

Extension of the Database

It is possible to extend the human database (but without the corresponding rat parameters) for an additional 19 drugs further assess method B with CL_{int} values for 52 drugs. These data were used to predict CL_{int} using the PB-SF (method A) and compared to CL_{int} calculated from *in vivo* data using either the well-stirred or the parallel tube liver model (Figs. 5A and 5B). Both observed and predicted values for the well-stirred model are also listed in Table I. Regression analysis using either the well-stirred or the parallel tube liver models, respectively, generated empirical scaling factors of 7.9 g protein/kg and 5.4 g protein/kg. Thus the extent of underestimation apparent with the use of method A to predict *in vivo* CL_{int} is approximately 9- and 6-fold, depending on the liver model used.

Effects of Plasma Protein Binding

Figure 5C shows the prediction of human CL_{int} for 52 drugs without incorporating plasma protein binding (using the well-stirred model). Compared with the prediction using PB-SF with plasma protein binding incorporated (Fig. 5A), the bias was reduced by ignoring the plasma protein binding, but the precision was also reduced.

Figure 6 compares nonspecific drug binding in plasma and microsomal matrices, the $f_{u,m}$ at a microsomal protein concentration of 1 mg/ml is plotted against the $f_{u,p}$ (plasma protein concentration 40 mg/ml). The lines shown are based on Eq. 18 and either assume equality in binding ($K_{a,m}/K_{a,p}$ ratio of unity) or refer to the $K_{a,m}/K_{a,p}$ ratio obtained by regression analysis. Only for neutral drugs were K_a values similar between microsomes and plasma ($K_{a,m}/K_{a,p}$ ratio = 1.02). For basic drugs and acidic drugs the $K_{a,m}$ was higher (average $K_{a,m}/K_{a,p}$ ratio 8.7) or lower (average $K_{a,m}/K_{a,p}$ ratio 0.022), respectively.

DISCUSSION

In order to assess various approaches to predicting human *in vivo* clearance a data base of 52 drugs has been collated from a variety of literature sources. Comparisons published previously have focused on a relatively small number of drugs (3,7,11) and have been less comprehensive in the range of approaches investigated. The present analysis considers primarily *in vitro* and *in vivo* CL_{int} values, the latter obtained from “deconstructing” CL_h to generate a wide range of parameter values (4 orders of magnitude) to allow detailed comparisons. Also considered is the prediction of CL_h .

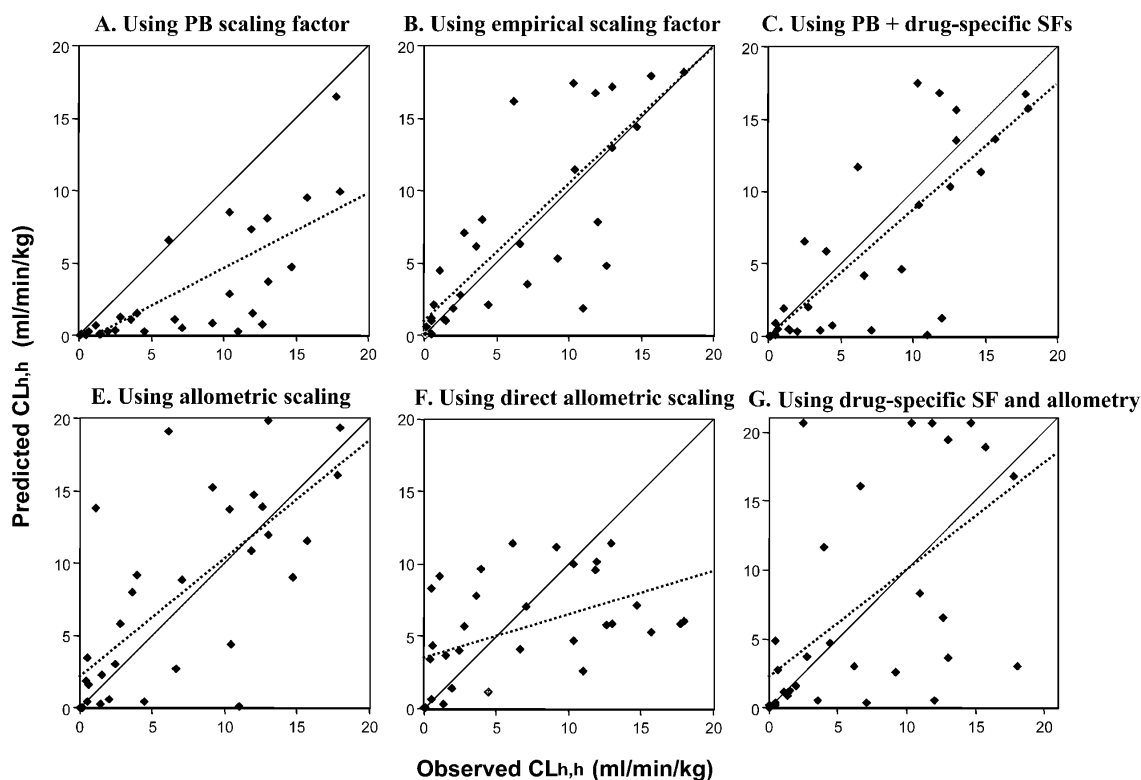


Fig. 3. Correlations between the observed and predicted human CL_h for 33 drugs determined using six different approaches. (A) Using PB-SF, (B) using empirical SF, (C) using PB-SF and drug-specific SF, (E) using allometric scaling, (F) direct allometric scaling, and (G) Using drug-specific SF and allometry. Lines represent the regression (dotted line) and unity (solid line).

Fig. 1C, it provided no improvement in the precision of the prediction over the use of human *in vitro* data alone.

A similar picture was obtained from consideration of CL_h prediction using the five approaches to determining CL_{int} and the well-stirred liver model. Human microsomal derived CL_{int} again provided the most accurate predictions of CL_h . The two further methods were investigated for CL_h prediction, using allometry from rat CL_h directly as well as in combination with a drug-specific factor. Once again, neither of these options provided an improvement on the use of *in vitro* microsomal parameters.

The bias of a prediction is of importance as well as the precision. Using the PB approach (based on microsomal enzyme recovery) to scale *in vitro* CL_{int} to provide *in vivo* CL_{int} values results in a systematic underprediction. The selection of the particular liver model used to “deconstruct” CL_h to give an *in vivo* CL_{int} influences the extent to which this occurs. This is because the parallel tube model always gives lower *in vivo* CL_{int} values than the well-stirred liver model and the dispersion model gives intermediate values (34). In a recent analysis of the use of liver models for prediction of rat clearances from both hepatocytes and hepatic microsomes it was concluded that there was the minimal differences between the liver models. Thus the simplest, most commonly adopted, well-stirred liver model could continue to be used with confidence (34).

The bias seen with *in vitro* data can be reduced or removed by a number of alternative procedures. Overall the use of an empirical scaling factors (method B) and the drug-specific method (method C) appear to be the best methods, as

they show lower bias than the PB scaling factor and better precision than the allometric approaches. The use of *in vitro* human microsomal data with an empirical scaling factor (method B) may be regarded as preferable, as it does not require extra information from preclinical studies both *in vitro* and *in vivo*.

The decision of whether to incorporate plasma protein binding in clearance prediction is controversial. Whereas a basic tenet of physiologically based pharmacokinetics is that the unbound drug concentration in the plasma dictates tissue distribution, there have been reports that *in vitro* clearance provides a better estimate of *in vivo* clearance of total rather than unbound drug concentration (7,35,36). Ignoring plasma binding in the present analysis provides a good example of how the bias can be removed from a prediction but only at the expense of a loss in precision. A further variant on this idea is the relative role of drug binding in plasma and hepatic microsomes. It is an attractive option (7) to consider that the parameters describing the two processes may cancel out in the liver model calculation, and hence neither process needs to be measured. However it is clear from the comparative analysis of microsomal and plasma binding presented here that drug binding within these two matrices is unlikely to be equivalent and hence should not be cancelled out in principle.

The fraction unbound in either matrix is dependent upon protein/lipid (binding sites) concentration and K_a values. For plasma, albumin is usually the major site of drug binding but within the microsomal matrix the high content of lipid provides potential binding sites in addition to protein. In the analysis presented here protein is taken as the common bind-

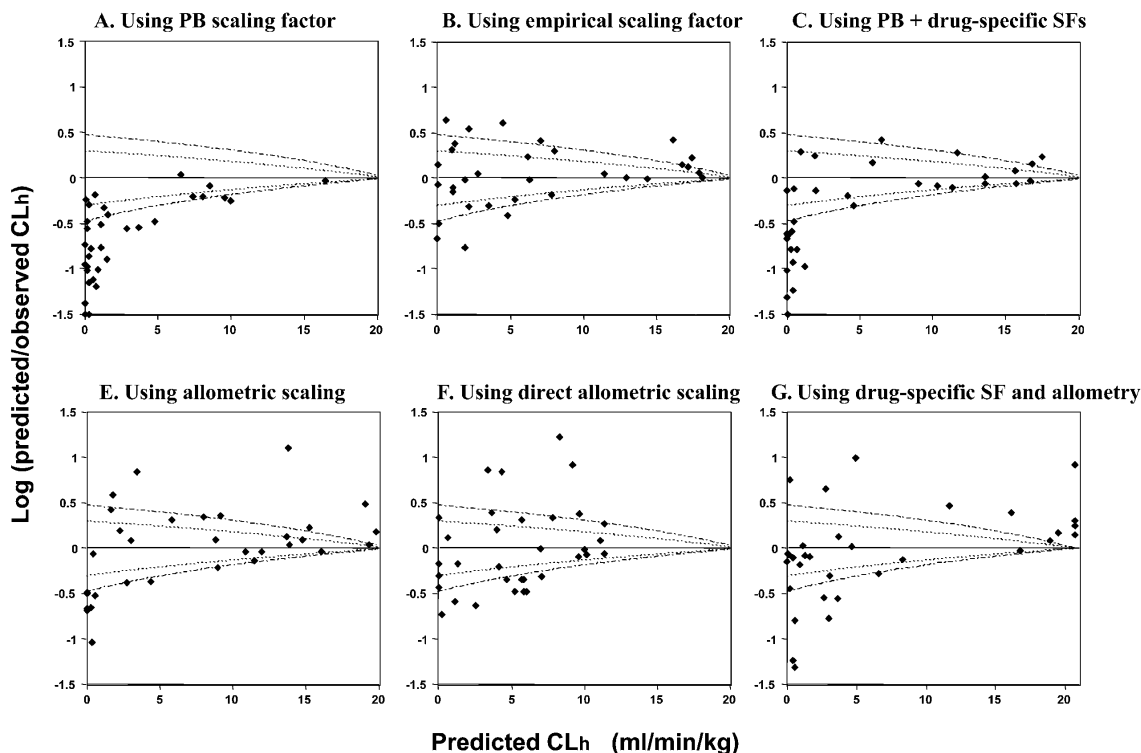


Fig. 4. Precision error (expressed as the log of the predicted/observed CL_h ratio) for predicted CL_h for 33 drugs using six different approaches. (A) Using PB-SF, (B) using empirical SF, (C) using PB-SF and drug-specific SF, (E) using allometric scaling, (F) direct allometric scaling, and (G) using drug-specific SF and allometry. The light and heavy dotted lines indicate the limits for the CL_h prediction when either a 2- or 3-fold error, respectively, on the CL_{int} prediction propagated into CL_h .

ing site in both matrices to illustrate the potential difference between plasma and microsomes. Plotting the unbound fraction in microsomes (at the protein concentration of 1 mg/ml) against the unbound fraction in plasma (40 g/ml) indicates that only in the case of neutral drugs are the affinity constants comparable. However $f_{u,m}$ differs from $f_{u,p}$ because of difference in protein concentration. In order to achieve a similar fraction unbound in microsomes (commonly used protein concentration of 1 mg/ml) and plasma the microsomal K_a

should exceed plasma by 40-fold. Using nonlinear regression a clear difference between the affinity constants in the two matrices can be quantified for bases ($K_{a,m} > K_{a,p}$ by 8.7) and for acids ($K_{a,p} > K_{a,m}$ by 45). The substantial difference in K_a observed for bases probably reflects the extensive binding of these drugs to lipid whereas for acids the nature and concentration of protein dominates. For the former class of drugs, $f_{u,m}$ will coincide with $f_{u,p}$ if a microsomal suspension of approximately 5 mg/ml protein concentration is used.

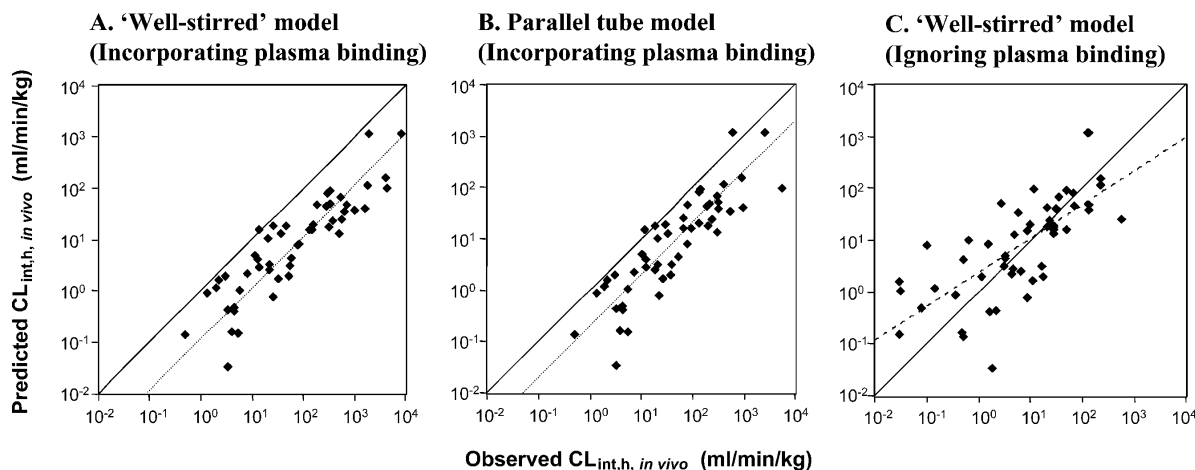


Fig. 5. Correlation between the observed and predicted human CL_{int} for a dataset of 52 drugs using the PB scaling factor based on microsomal recovery and two different liver models [well-stirred (panels A and C) and parallel tube (panel B) models]. Plasma protein binding was incorporated in panels A and B and ignored in panel C. Lines represent the regression with a fixed (A, B) or non-fixed (C) slope (dotted) and unity (solid).

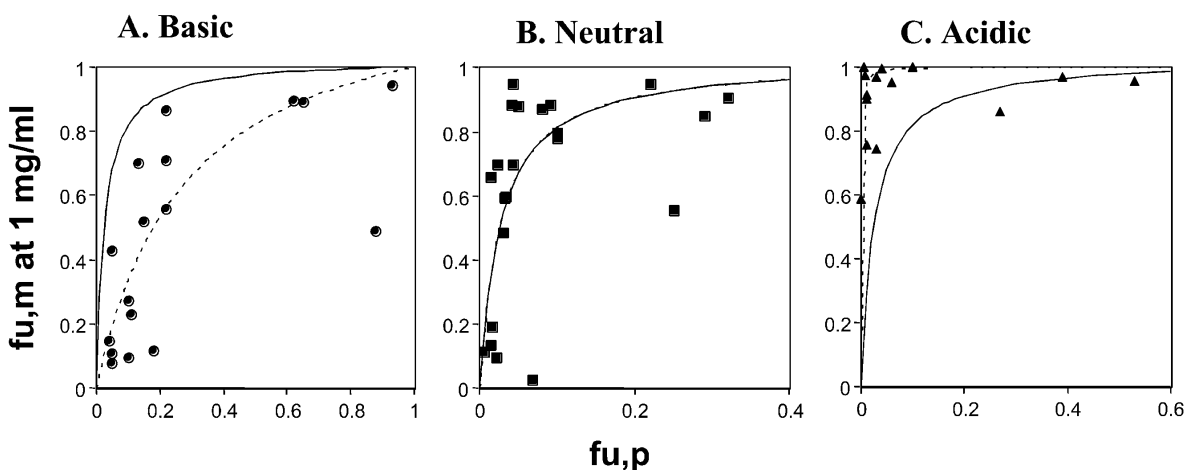


Fig. 6. Relationship between nonspecific binding of basic (panel A), neutral (panel B), and acidic (panel C) drugs in microsomes and plasma. The $f_{u,m}$ values refer to a protein concentration of 1 mg/ml and $f_{u,p}$ to 40 mg/ml. Solid lines represent the simulated lines based on Eq. 18 assuming the same affinity constant in plasma and microsomes, and dotted lines represent the simulations using microsome/plasma affinity constant ratios of 8.7 (panel A), 1.02 (panel B), and 0.022 (panel C) obtained by nonlinear regression.

The use of an empirical SF (method B) to overcome the bias in prediction increases value of the scaling factor over the PB value determined from microsomal recovery (0.86 g protein/kg) to a value of 7.9 g protein/kg. While this provides an immediate, pragmatic solution for systematic underprediction, in the longer term it is important to identify explanations and modify scaling strategies to account for these confounding issues. Previous analyses of rat predictions from both hepatocytes and hepatic microsomes did not show a systematic bias (2,34). This undoubtedly reflects the genetic and environmental constancy that operates with animal experimentation. Thus the drug metabolizing enzymes isolated and monitored *in vitro* are essentially identical to those operating *in vivo*. For human tissue experimentation there is an impact from extrinsic factors such as tissue handling and storage procedures (often not detailed) that may increase variability *in vitro* beyond that evident *in vivo*. Substantial inter-individual variability in drug clearance is well known and the mismatch between the liver donors and the young healthy volunteers used for most *in vivo* studies are important. The systematic underprediction of human CL_{int} from *in vitro* human hepatic microsomal studies may be, at least in part, a reflection of this situation.

A number of factors are of more importance for human than rat clearance studies. One is the role of CYP3A enzymes, the most abundant and most used subfamily of human enzymes. Their atypical kinetics and propensity to activation phenomena are important considerations for clearance predictions (37). Also the expression of these enzymes extrahepatically may have a major impact (38–40). Until the relative importance of the above factors, amongst others, to the overall underprediction phenomenon is established a pragmatic approach of adopting an empirical SF is recommended.

REFERENCES

1. J. B. Houston. Utility of *in vitro* drug metabolism data in predicting *in vivo* metabolic clearance. *Biochem. Pharmacol.* **47**: 1469–1479 (1994).
2. J. B. Houston and D. J. Carlile. Prediction of hepatic clearance from microsomes, hepatocytes, and liver slices. *Drug Metab. Rev.* **29**:891–922 (1997).
3. T. Iwatsubo, N. Hirota, T. Ooie, H. Suzuki, N. Shimada, K. Chiba, T. Ishizaki, C. E. Green, C. A. Tyson, and Y. Sugiyama. Prediction of *in vivo* drug metabolism in the human liver from *in vitro* metabolism data. *Pharmacol. Ther.* **73**:147–171 (1997).
4. H. Boxenbaum. Interspecies scaling, allometry, physiological time, and the ground plan of pharmacokinetics. *J. Pharmacokin. Biopharm.* **10**:201–227 (1982).
5. F. Gaspari and M. Bonati. Interspecies metabolism and pharmacokinetic scaling of theophylline disposition. *Drug Metab. Rev.* **22**:179–207 (1990).
6. I. Mahmood and J. D. Balian. Interspecies scaling: predicting clearance of drugs in humans. Three different approaches. *Xenobiotica* **9**:887–895 (1996).
7. R. S. Obach, J. G. Baxter, T. E. Liston, B. M. Silber, B. C. Jones, F. MacIntyre, D. J. Rance, and P. Wastall. The prediction of human pharmacokinetic parameters from preclinical and *in vitro* metabolism data. *J. Pharmacol. Exp. Ther.* **283**:46–58 (1997).
8. W. L. Chiou, G. Robbie, S. M. Chung, T.-C. Wu, and C. Ma. Correlation of plasma clearance of 54 extensively metabolized drugs between humans and rats: Mean allometric coefficient of 0.66. *Pharm. Res.* **15**:1474–1479 (1998).
9. Y. Naritomi, S. Terashita, S. Kimura, A. Suzuki, A. Kagayama, and Y. Sugiyama. Prediction of human hepatic clearance from *in vivo* animal experiments and *in vitro* metabolic studies with liver microsomes from animals and humans. *Drug Metab. Dispos.* **29**: 1316–1324 (2001).
10. T. Lave, S. Dupin, C. Schmitt, R. C. Chou, D. Jaeck, and P. Coassolo. Integration of *in vitro* data into allometric scaling to predict hepatic metabolic clearance in man: Application to 10 extensively metabolized drugs. *J. Pharm. Sci.* **86**:584–590 (1997).
11. J. Zuegge, G. Schneider, P. Coassolo, and T. Lave. Prediction of hepatic metabolic clearance: Comparison and assessment of prediction models. *Clin. Pharmacokin.* **40**:553–563 (2001).
12. D. J. Carlile, N. Hakooz, M. K. Bayliss, and J. B. Houston. Microsomal prediction of *in vivo* clearance of CYP2C9 substrate in human. *Br. J. Clin. Pharmacol.* **47**:625–635 (1999).
13. A. J. Stevens, S. W. Martin, B. S. Brennan, A. McLachlan, L. A. Gifford, M. Rowland, and J. B. Houston. Regional drug delivery II: relationship between drug targeting index and pharmacokinetic parameters for three non-steroidal anti-inflammatory drugs using the rat air pouch model of inflammation. *Pharm. Res.* **12**: 1987–1996 (1995).
14. R. S. Obach. Prediction of human clearance of twenty-nine drugs from hepatic microsomal intrinsic clearance data: An examination of *in vitro* half-life approach and nonspecific binding to microsomes. *Drug Metab. Dispos.* **27**:1350–1359 (1999).

15. T. Iwatsubo, H. Suzuki, and Y. Sugiyama. Prediction of species differences (rats, dogs, humans) in the *in vivo* metabolic clearance of YM796 by the liver from *in vitro* data. *J. Pharmacol. Exp. Ther.* **283**:462–469 (1997).
16. M. Chiba, M. Hensleigh, and J. H. Lin. Hepatic and intestinal metabolism of indinavir, an HIV protease inhibitor, in rat and human microsomes. Major role of CYP3A. *Biochem. Pharmacol.* **53**:1187–1195 (1997).
17. S. K. Balani, E. J. Woolf, V. L. Hoagland, M. G. Sturgill, P. J. Deutsch, K. C. Yeh, and J. H. Lin. Disposition of indinavir, a potent HIV-1 protease inhibitor, after an oral dose in humans. *Drug Metab. Dispos.* **24**:1389–1394 (1996).
18. J. H. Lin, M. Chiba, S. K. Balani, I.-W. Chen, G. Y.-S. Kwei, K. J. Vastag, and J. A. Nishime. Species differences in the pharmacokinetics and metabolism of indinavir, a potent human immunodeficiency virus protease inhibitor. *Drug Metab. Dispos.* **24**:1111–1120 (1996).
19. R. J. Parker, J. M. Collins, and J. M. Strong. Identification of 2,6-xylylidine as a major lidocaine metabolite in human liver slices. *Drug Metab. Dispos.* **24**:1167–1173 (1996).
20. C. M. Dixon, P. V. Colthup, C. J. Serabjit-Singh, B. M. Kerr, C. C. Boehlert, G. R. Park, and M. H. Tarbit. Multiple forms of cytochrome P450 are involved in the metabolism of ondansetron in humans. *Drug Metab. Dispos.* **23**:1225–1230 (1995).
21. G. Engel, U. Hofmann, H. Heidemann, J. Cosme, and M. Eichelbaum. Antipyrine as a probe for human oxidative drug metabolism: identification of the cytochrome P450 enzymes catalyzing 4-hydroxyantipyrine, 3-hydroxymethylantipyrine, and norantipyrine formation. *Clin. Pharmacol. Ther.* **59**:613–623 (1996).
22. J. C. Bloomer, S. E. Clarke, and R. J. Chenery. Determination of P4501A2 activity in human liver microsomes using [3-14C-methyl]caffeine. *Xenobiotica* **25**:917–927 (1995).
23. U. G. Eriksson, J. Lundahl, C. Baarnhielm, and C. G. Regardh. Stereoselective metabolism of felodipine in liver microsomes from rat, dog, and human. *Drug Metab. Dispos.* **19**:889–894 (1991).
24. S. V. Otton, E. M. Gillam, M. S. Lennard, G. T. Tucker, and H. F. Woods. Propranolol oxidation by human liver microsomes—the use of cumene hydroperoxide to probe isoenzyme specificity and regio- and stereoselectivity. *Br. J. Clin. Pharmacol.* **30**:751–760 (1990).
25. R. Ishida, S. Obara, Y. Masubuchi, S. Narimatsu, S. Fujita, and T. Suzuki. Induction of propranolol metabolism by the azo dye sudan III in rats. *Biochem. Pharmacol.* **43**:2489–2492 (1992).
26. D. B. Jones, M. S. Ching, R. A. Smallwood, and D. J. Morgan. A carrier-protein receptor is not a prerequisite for avid hepatic elimination of highly bound compounds: A study of propranolol elimination by the isolated perfused rat liver. *Hepatology* **5**:590–593 (1985).
27. K. S. Pang and M. Rowland. Hepatic clearance of drugs. I. Theoretical considerations of a “well-stirred” model and a “parallel tube” model. Influence of hepatic blood flow, plasma and blood cell binding, and the hepatocellular enzymatic activity on hepatic drug clearance. *J. Pharmacokin. Biopharm.* **5**:625–653 (1977).
28. R. L. Dedrick. Animal scale-up. *J. Pharmacokin. Biopharm.* **1**:435–461 (1973).
29. K. B. Bischoff, R. L. Dedrick, D. S. Zaharko, and J. A. Longstreth. Methotrexate pharmacokinetics. *J. Pharm. Sci.* **60**:1128–1133 (1971).
30. G. M. Pollack, K. L. R. Brouwer, K. B. Demby, and J. A. Jones. Determination of hepatic blood flow in the rat using sequential infusions of indocyanine green or galactose. *Drug Metab. Dispos.* **18**:197–202 (1999).
31. K. S. Pang and J. R. Gillette. Complications in the estimation of hepatic blood flow *in vivo* by pharmacokinetic parameters. *Drug Metab. Dispos.* **6**:567–576 (1978).
32. L. B. Sheiner and S. L. Beal. Some suggestions for measuring predictive performance. *J. Pharmacokin. Biopharm.* **9**:503–512 (1981).
33. M. G. Soars, B. Burchell, and R. J. Riley. *In vitro* analysis of human drug glucuronidation and prediction of *in vivo* metabolic clearance. *J. Pharmacol. Exp. Ther.* **301**:382–390 (2002).
34. K. Ito and J. B. Houston. Comparison of the use of liver models for predicting drug clearance using *in vitro* kinetic data from hepatic microsomes and isolated hepatocytes. *Pharm. Res.* **21**:785–792 (2004).
35. R. J. Riley. The potential pharmacological and toxicological impact of P450 screening. *Curr. Opin. Drug Discov. Dev.* **4**:45–54 (2001).
36. P. Poulin and F-P Theil. Prediction of pharmacokinetics prior to *in vivo* studies. II. Generic physiologically based pharmacokinetic models for drug disposition. *J. Pharm. Sci.* **91**:1358–1370 (2002).
37. J. B. Houston and K. E. Kenworthy. *In vitro-in vivo* scaling of CYP kinetic data not consistent with the classical Michaelis-Menten model. *Drug Metab. Dispos.* **28**:246–254 (2000).
38. M. F. Paine, M. Khalighi, J. M. Fisher, D. D. Shen, K. L. Kunze, C. L. Marsh, J. D. Perkins, and K. E. Thummel. Characterization of interintestinal and intrainestinal variations in human CYP3A-dependent metabolism. *J. Pharmacol. Exp. Ther.* **283**:1552–1562 (1997).
39. Q. Y. Zhang, D. Dunbar, A. Ostrowska, S. Zeisloft, J. Yang, and L. S. Kaminsky. Characterization of human small intestinal cytochromes P-450. *Drug Metab. Dispos.* **27**:804–809 (1999).
40. H. J. Lin, M. Chiba, and T. A. Baillie. Is the role of the small intestine in first-pass metabolism overemphasized? *Pharmacol. Rev.* **51**:135–157 (1999).